Terahertz dynamics of photogenerated carriers in ferromagnetic InGaMnAs

G. A. Khodaparast, D. C. Larrabee, and J. Kono[a)]
Department of Electrical and Computer Engineering, Rice Quantum Institute, and Center for Nanoscale Science and Technology, Rice University, Houston, Texas 77005

D. S. King
Department of Applied Physics, Stanford University, Stanford, California 94305

J. Kato
Department of Applied Physics and Physico-Infomatics, Keio University, Yokohama, Kanagawa 223-8522, Japan

T. Slupinski,[b)] A. Oiwa, and H. Munekata
KAST and Imaging Science and Engineering Laboratory, Tokyo Institute of Technology, Yokohama, Kanagawa 226-8503, Japan

G. D. Sanders and C. J. Stanton
Department of Physics, University of Florida, Gainesville, Florida 32611

(Presented on 15 November 2002)

We have measured the picosecond transient carrier response of InGaMnAs/InP by two-color pump–probe spectroscopy, using an intense near-infrared beam as the pump and a 52.5 μm (5.7 THz) beam as the probe. We observed strongly nonexponential decays, especially at high pump fluences and low temperatures, where a pronounced dip developed in the terahertz differential transmission. This dip disappeared at the highest fluence where a transmission plateau versus time delay was observed. Our band structure calculations suggest that this intriguing behavior may be due to carrier dynamics associated with Γ–L intervalley scattering that becomes efficient when ferromagnetism modifies the band structure. © *2003 American Institute of Physics.* [DOI: 10.1063/1.1555375]

The advent of III–V magnetic semiconductors has opened up new possibilities for exploring spin-dependent phenomena as well as fabricating devices based on both the charge and spin degrees of freedom of electrons. In particular, the discovery of carrier-induced ferromagnetism has provided a unique system for studying the physics of itinerant carriers interacting with localized Mn spins.[1–5] Although electrical transport and magnetic properties have been extensively investigated, there has been limited success in exploring the optical properties of (III, Mn)V systems.[6–9]

We have measured the picosecond transient carrier response of InGaMnAs/InP (Ref. 10) by two-color pump–probe spectroscopy at different temperatures and pump intensities. We used an intense picosecond pulse of near-infrared (NIR) radiation to create a large density of nonequilibrium carriers, which modifies the transmission and reflection of a delayed pulse of terahertz (THz) radiation. Our measurements demonstrate that the THz response of the transient carriers is very sensitive to both the temperature and pump intensity. In particular, at low temperatures and high pump intensities, we observed interesting substructure in carrier decay signals. Our band structure calculations based on a 30-band **k·p** model suggest that this behavior may be related to Γ–L intervalley scattering, which is possible only when the quasi-Fermi energy in the Γ valley becomes high enough. We speculate that band structure modifications due to ferromagnetic order at low temperatures are playing an important role in the observed effects.

We studied a lattice-matched ferromagnetic structure. It consisted of a 50 nm thick $(In_{0.53}Ga_{0.47})_{1-x}Mn_xAs$ magnetic layer on top of a 100 nm $In_{0.53}Ga_{0.47}As$ nonmagnetic buffer layer grown on an InP(001) substrate with a substrate temperature of 186 °C.[10] Typical hole densities and mobilities are $2-3\times10^{19}$ cm^{-3} and $\sim$20 cm^2/V s, respectively. A Curie temperature (T_c) of 100–120 K has been achieved in these structures for $x=0.13$, which is comparable to or higher than the highest T_c achieved in (Ga,Mn)As ($T_c=100-110$ K for $x\sim0.05$). Unlike the (Ga,Mn)As system, T_c does not saturate above 5% Mn content and increases in regions of high x. The magnetization easy axis is in the plane of the epilayer. The sample studied in this work had $x=0.13$ and a $T_c\sim110$ K.

The NIR source (pump laser) was a Ti:sapphire-based regenerative amplifier operating at 800 nm with a pulse width $\sim$1 ps. The THz source (probe laser) was the Stanford FEL, operating at 52.5 μm (5.7 THz) with a pulse width of $\sim$2 ps.[11] The NIR and THz beams were combined by a Pellicle plate and then focused onto the sample, which was placed in a helium flow cryostat with polypropylene windows. The measurements were performed in both transmission and reflection (45°) geometries. A liquid-helium-cooled Ge:Ga photoconductive detector with Si filter was used to detect the THz beam transmitted through or reflected from the sample.

a)Author to whom correspondence should be addressed; electronic mail: kono@rice.edu
b)Present address: Institute of Experimental Physics, Warsaw University, Hoza 69, 00-681 Warsaw, Poland.

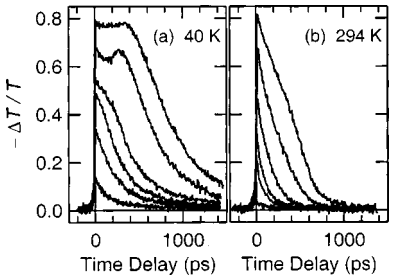

FIG. 1. THz transmission vs time delay at (a) 40 K and (b) 294 K for pump fluences of (from largest to smallest transmission change) 10, 4.0, 1.3, 0.6, 0.4, and 0.1 mJ/cm^2. The shoulder around 300 ps appears at low temperature and high pump fluence.

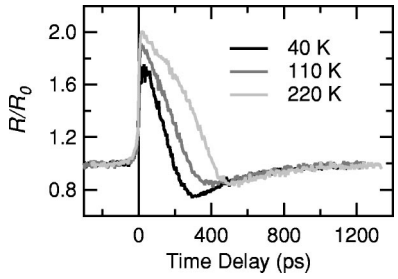

FIG. 3. Probe reflection vs time delay for the InGaMnAs sample for a pump fluence of 10 mJ/cm^2. Note that there is no peak in the reflectivity around 200 ps which could cause the dip in transmission.

Figures 1(a) and 1(b) show the differential transmission of THz radiation for the InGaMnAs sample as a function of time delay for a range of NIR pump fluences (10–0.1 mJ/cm^2) at (a) 40 and (b) 294 K. At the lowest temperature and fluence, the differential transmission jumps to 14% when the pump and probe coincide, then decays back to zero with a decay time of 100 ps. As the pump fluence is increased, the transmission jump and decay time get larger, up to 78% and 810 ps at the highest pump fluence. The transmission develops an interesting shoulder at higher fluences which is most pronounced at 4.0 mJ/cm^2, rising to roughly 10% above the low-intensity decay shape and situated at 250 ps. At 10 mJ/cm^2, the transmission does not begin to decrease until after the shoulder, at about 400 ps. At room temperature, the initial transmission change varies smoothly from 4% at 0.1 mJ/cm^2 to 81% at 10 mJ/cm^2, and the decay time from 100 to 400 ps. The shoulder is not present at room temperature except for a broad, shallow bump at 10 mJ/cm^2 centered around 400 ps. We performed detailed temperature and power dependence studies, and found that the initial transmission change stays roughly constant regardless of temperature and the decay time increases when the shoulder appears. The shoulder is present and about 10% high at temperatures of 220 K and below for 10 mJ/cm^2, and appears at lower fluences for temperatures around 110 K and below. In another sample with $x=0.13$ and $T_c \sim 80$ K, preliminary power and temperature dependence measurements indicated similar behavior, including the appearance of the shoulder at low temperatures and high fluences.

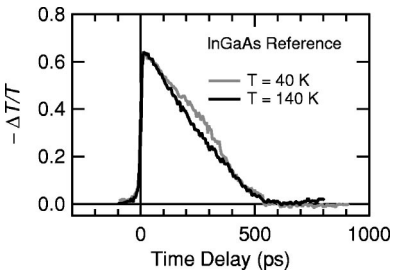

FIG. 2. Reference sample without InGaMnAs layer: THz transmission vs time delay at 40 and 140 K for a pump fluence of 10 mJ/cm^2 demonstrates the absence of the dip observed for the magnetic sample at high pump fluences and low temperatures [see Fig. 1(a)].

Measurements were also performed on a reference sample consisting of InGaAs(100 nm)/InP. Figure 2 shows the THz differential transmission of the reference sample as a function of time delay for a pump fluence of 10 mJ/cm^2 at 40 and 140 K. We observed a faster relaxation time in the reference sample than in the magnetic sample with weak temperature dependence. The absence of the shoulder at low temperature indicates that the features observed in the magnetic sample are due to the InGaMnAs layer.

Figure 3 shows the probe reflection as a function of time delay with the $T_c \sim 110$ K sample tilted 45° with respect to the incident beam, at a pump fluence of 10 mJ/cm^2 and a range of temperatures. There is no peak around 200 ps which might explain the appearance of a dip in transmission.

In order to better understand our observations, we performed calculations to model the band structure and allowed optical transitions. Our calculations are based on a 30 band **k·p** model[12–14] using the virtual crystal approximation for the InGaAs alloy, similar to work done on AlGaAs.[15] Results for $In_{0.53}Ga_{0.47}As$ give us a gap of ~0.8 eV, a Γ valley conduction band edge mass of $m^*=0.043m_0$, and a spin-orbit splitting of 0.37 eV. The minimum of the satellite L valley is about 0.7 eV above the Γ valley minimum.

Figure 4 shows the allowed optical transitions for an 800 nm pump (1.55 eV), which originate from each of the three valence bands: heavy hole, light hole, and spin-orbit-splitoff. The transition from the heavy hole to the Γ valley conduc-

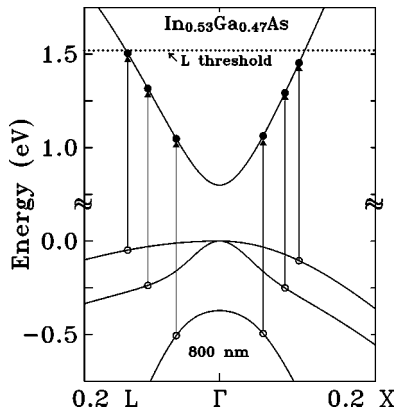

FIG. 4. Electronic structure for $In_{0.53}Ga_{0.47}As$ calculated from the 30 band **k·p** model. The conduction and valence bands are shown from the Γ point along the X and L directions to 0.2 of the zone edge. For photoexcitation by an 800 nm laser, three optical transitions are possible.

tion band is near the threshold for transfer to the satellite L valley. This allows the Γ electrons to scatter back and forth from the L valley.[16] This effect may be more pronounced at high pump intensities, giving rise to additional structure in the differential transmission plots. In addition, Mn doping may create electrons which are energetically able to scatter into the L valley.

The authors gratefully acknowledge support from NSF DMR-0134058 (CAREER), DARPA MDA972-00-1-0034, and AFOSR F49620-00-1-0349. C.J.S. would like to acknowledge Grant No. DE-FG02-02ER45984. H.M. would like to acknowledge partial support from Science Research in Priority Areas ''Semiconductor Nanospintronics'' of the Ministry to ECSST, Japan. We are grateful to H. A. Schwettman, T. I. Smith, R. L. Swent, T. Kimura, G. A. Marcus, M. Galt, D. Keegan, and B. Armstrong for their technical support during this work at the Stanford Picosecond Free Electron Laser Center.

[1] H. Munekata, H. Ohno, S. von Molnar, A. Segmuller, L. L. Chang, and L. Esaki, Phys. Rev. Lett. **63**, 1849 (1989).
[2] H. Munekata, H. Ohno, R. R. Ruf, R. J. Gambino, and L. L. Chang, J. Cryst. Growth **111**, 1011 (1991).
[3] H. Ohno, H. Munekata, T. Penney, S. von Molnar, and L. L. Chang, Phys. Rev. Lett. **68**, 2664 (1992).
[4] H. Munekata, A. Zaslavsky, P. Fumagalli, and R. J. Gambino, Appl. Phys. Lett. **63**, 2929 (1993).
[5] H. Ohno, A. Shen, F. Matsukura, A. Oiwa, A. Endo, S. Katsumoto, and Y. Iye, Appl. Phys. Lett. **69**, 363 (1996).
[6] B. Beschoten, P. A. Crowell, I. Malajovich, D. D. Awschalom, F. Matsukura, A. Shen, and H. Ohno, Phys. Rev. Lett. **83**, 3073 (1999).
[7] E. J. Singley, R. Kawakami, D. D. Awschalom, and D. N. Basov, Phys. Rev. Lett. **89**, 097203 (2002).
[8] J. Wang, G. A. Khodaparast, J. Kono, T. Slupinski, A. Oiwa, and H. Munekata, in J. Superconduct. (see also cond-mat/0207563).
[9] M. A. Zudov, J. Kono, Y. H. Matsuda, T. Ikaida, N. Miura, H. Munekata, G. D. Sanders, Y. Sun, and C. J. Stanton, Phys. Rev. B **66**, 161307R (2002).
[10] T. Slupinski, H. Munekata, and A. Oiwa, Appl. Phys. Lett. **80**, 1592 (2002).
[11] J. Kono, A. H. Chin, A. P. Mitchell, T. Takahashi, and H. Akiyama, Appl. Phys. Lett. **75**, 1119 (1999); M. A. Zudov, J. Kono, A. P. Mitchell, and A. H. Chin, Phys. Rev. B **64**, 121204(R) (2001); M. A. Zudov, A. P. Mitchell, A. H. Chin, and J. Kono, cond-mat/0209047.
[12] M. Cardona and F. H. Pollak, Phys. Rev. **142**, 530 (1966).
[13] D. W. Bailey, C. J. Stanton, and K. Hess, Phys. Rev. B **42**, 3423 (1990).
[14] C. J. Stanton, D. W. Bailey, and K. Hess, Phys. Rev. Lett. **65**, 231 (1990).
[15] M. Ulman, D. W. Bailey, L. H. Acioli, F. G. Vallee, C. J. Stanton, E. P. Ippen, and J. G. Fujimoto, Phys. Rev. B **47**, 10267 (1993).
[16] C. J. Stanton and D. W. Bailey, Phys. Rev. B **45**, 8369 (1992).